



Influence of CdCl₂ activation treatment on ultra-thin Cd_{1-x}Zn_xS/CdTe solar cells



A.J. Clayton^{a,*}, M.A. Baker^b, S. Babar^b, P.N. Gibson^c, S.J.C. Irvine^a, G. Kartopu^a, D.A. Lamb^a, V. Barrioz^a

^a Centre for Solar Energy Research, Glyndŵr University, OptIC, St. Asaph LL17 0JD, UK

^b Faculty of Engineering & Physical Sciences, University of Surrey, Guildford GU2 7XH, UK

^c Institute for Health & Consumer Protection, Joint Research Centre, 21020 Ispra, VA, Italy

ARTICLE INFO

Article history:

Received 3 November 2014

Received in revised form 28 July 2015

Accepted 28 July 2015

Available online 5 August 2015

Keywords:

Metal-organic chemical vapor deposition

Thin films

Cadmium telluride

Photovoltaics

X-ray photoelectron spectroscopy

X-ray diffraction

ABSTRACT

Ultra-thin CdTe photovoltaic solar cells with an absorber thickness of 0.5 μm were produced by metal organic chemical vapour deposition onto indium tin oxide coated boroaluminosilicate glass. A wide band gap Cd_{1-x}Zn_xS alloy window layer was employed to improve spectral response in the blue region of the solar spectrum. X-ray photoelectron spectroscopy, X-ray diffraction and scanning electron microscopy were used to monitor changes in the chemical composition and microstructure of the Cd_{1-x}Zn_xS/CdTe solar cell after varying the post-deposition CdCl₂ activation treatment time and annealing temperature. The CdCl₂ treatment leached Zn from the Cd_{1-x}Zn_xS layer causing a redshift in the spectral response onset of window absorption. S diffusion occurred across the Cd_{1-x}Zn_xS/CdTe interface, which was more pronounced as the CdCl₂ treatment was increased. A CdTe_{1-y}S_y alloy was formed at the interface, which thickened with CdCl₂ treatment time. Small concentrations of S (up to 2 at.%) were observed throughout the CdTe layer as the degree of CdCl₂ treatment was increased. Greater S diffusion across the Cd_{1-x}Zn_xS/CdTe interface caused the device open-circuit voltage (*V*_{oc}) to increase. The higher *V*_{oc} is attributed to enhanced strain relaxation and associated reduction of defects in the interface region as well as the increase in CdTe grain size.

© 2015 Elsevier B.V. All rights reserved.

1. Introduction

CdTe solar module production is the most successful thin film technology for commercial photovoltaics (PV) [1]. This has much to do with the relative ease of industrial scale-up [2] as well as its near optimum band gap for solar absorption [3]. Recent developments led by industry have resulted in improvements to world records for both cell (21.0% over area of 1.06 cm²) and module (17.5%) conversion efficiencies [4]. In order to produce CdTe solar cells without the effects of pinholes, the absorber thickness is typically 2–7 μm [5,6], but the majority of photons are absorbed in the first 1 μm [7,8]. However, the performance of ultra-thin CdTe solar cells (absorber thickness ≤ 1 μm) can be optically limited with loss of longer wavelength photons towards the CdTe band gap [8–10]. For future large scale production of CdTe solar modules to remain sustainable, consideration has to be given to the global availability of tellurium [1,8,11]. Hence, there is currently great interest in improving the performance of ultra-thin CdTe solar cells.

Ultra-thin CdTe solar cells can be susceptible to a drop in open circuit voltage (*V*_{oc}) and fill factor (*FF*) [12,13]. For the latter, this is typically associated with an increased number of micro-shunts [9,13] due to

the ultra-thin CdTe absorber layer having a large density of pinholes. It has also been suggested [14] that recombination at the back contact becomes more prominent when reducing the CdTe absorber thickness for ultra-thin solar cells, which has an adverse effect on *V*_{oc}. In addition, reports have shown [13,15] that ultra-thin CdTe solar cells are more sensitive to the effects of CdCl₂ activation treatment, which can significantly affect the wide band gap Cd_{1-x}Zn_xS alloy window layer composition.

It has been demonstrated [15] that the CdCl₂ layer deposited prior to the annealing treatment needs to be sufficiently thick to induce an appropriate level of intermixing across the Cd_{1-x}Zn_xS/CdTe interface in order to reduce strain related defects for enhancement of the *V*_{oc}. This study uses X-ray photoelectron spectroscopy (XPS), X-ray diffraction (XRD) and scanning electron microscopy (SEM) to examine in detail the compositional and structural changes to ultra-thin Cd_{1-x}Zn_xS/CdTe solar cells after different levels of CdCl₂ activation treatment. The changes in individual layer and interface compositions following the different CdCl₂ activation treatments have been correlated with device PV properties.

2. Experimental

Ultra-thin Cd_{1-x}Zn_xS/CdTe solar cells were produced using metal organic chemical vapour deposition (MOCVD) in a single growth chamber.

* Corresponding author.

E-mail address: a.clayton@glyndwr.ac.uk (A.J. Clayton).

Boroaluminosilicate glass coated with indium tin oxide (ITO) was used as the substrate, with glass thickness of 1.1 mm and an ITO sheet resistance of 4–8 Ω/sq . The ultra-thin CdTe solar cell spectral response in the blue region of the solar spectrum was enhanced by using a wide band gap $\text{Cd}_{1-x}\text{Zn}_x\text{S}$ window layer, 0.24 μm in thickness [5,13,16]. As was used as the CdTe acceptor dopant with concentration [As] in the range of $\sim 10^{18}$ – 10^{19} atoms/ cm^3 . An in situ CdCl_2 treatment process [17] was used with variable deposition time for control of the relative CdCl_2 layer thickness and hence level of Cl diffusion into the CdTe layer during anneal at 420 °C for activation of the solar cell. A CdTe absorber thickness of 0.5 μm was employed for all ultra-thin solar cells due to high sensitivity of the spectral response to the CdCl_2 activation treatments. Each ultra-thin CdTe solar cell device consisted of $8 \times 0.25 \text{ cm}^2$ cells defined by evaporating Au through a shadow mask.

Compositional changes to the ultra-thin $\text{Cd}_{1-x}\text{Zn}_x\text{S}/\text{CdTe}$ solar cells were determined by using a Thermo Scientific Thetaprobe XPS instrument employing a monochromatic Al K_{α} X-ray source with a photon energy of 1486.7 eV. The diameter of the X-ray beam spot was 800 μm . Wide scan spectra were recorded at a pass energy of 300 eV and narrow scan spectra recorded at pass energy of 20 eV. Quantification of the XPS data was performed after a Shirley background subtraction using the Thermo Scientific Avantage software which employs instrument modified Wagner sensitivity factors. Depth profiling was undertaken using an Ar^+ ion gun operating at 3 keV and current density of 11.1 $\mu\text{A}/\text{cm}^2$ (1 μA induced beam current, rastered over a $3 \times 3 \text{ mm}^2$ area). Spectra were charge referenced to the C 1 s peak at 285.0 eV.

XRD analysis was carried out with a Bruker D8 Discover instrument, equipped with twin primary and secondary optics. Copper K_{α} radiation was used, together with a Lynx-eye position sensitive detector. All scans reported here were made in the para-focussing mode due to instrumental resolution being much higher than in the parallel beam mode. Following data collection, the instrumental software was used to strip the $K_{\alpha 2}$ component from the diffraction patterns. XRD peak fitting was based on the least-squares fitting of broadened peaks to a pseudo-Voigt function enabling the grain size to be estimated from the Lorentzian component based on the Scherrer equation [18,19]. SEM was performed using a Jeol JSM-7100 F instrument, employing a Schottky field emission gun, operated at 10 keV.

Current density–voltage (J – V) measurements were carried out at AM1.5 using an Abet Technologies Ltd. solar simulator with light power density output equal to 100 mW/cm^2 calibrated using a Fraunhofer c-Si reference cell. Only single pass illumination from the front side of the cell was carried out with no intentional back reflection, but with possibility of this occurring from the Au back contacts. External quantum efficiency (EQE) measurements were carried out using a Bentham spectral response spectrometer under unbiased conditions over the spectral range of 0.3–1.0 μm .

3. Results and discussion

The different times (s) for the CdCl_2 layer deposition and 420 °C anneal used for the activation treatment of the ultra-thin CdTe solar cell devices are outlined in Table 1. Pre-anneal CdCl_2 layer thickness ranged from 0.9–2.0 μm between 80 and 179 s deposition time,

Table 1
The different CdCl_2 activation treatment parameters employed for ultra-thin CdTe solar cells.

Device	CdCl_2 (s)	Anneal (s)
Baseline	359	600
T179A10	179	600
T120A10	120	600
T080A10	80	600
T080A02	80	120
Reference	0	0

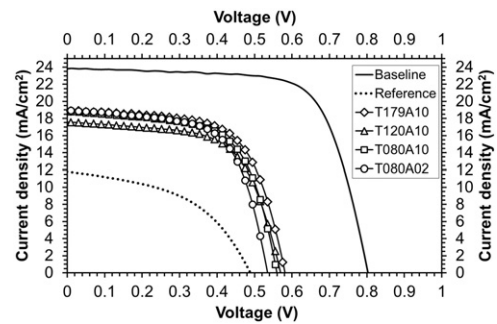


Fig. 1. J – V curves for cells from ultra-thin CdTe PV devices after CdCl_2 activation treatment; comparison to a baseline CdTe PV cell and reference ultra-thin PV cell.

respectively, based on a growth rate of 11 nm/s at 420 °C [17]. The treatment parameters typical for a solar cell device with baseline-MOCVD CdTe thickness of 2.25 μm are also shown. No ultra-thin device which has only received the high temperature anneal has been included in this study. A previous study [20] showed that annealing induces inter-diffusion, but that without the presence of CdCl_2 , the effects were not as prominent. The study reported here focuses on the effects of the CdCl_2 activation treatment only.

3.1. J – V and EQE curves

J – V curves for best cells from two ultra-thin CdTe PV devices having received the largest variation in CdCl_2 treatment are given in Fig. 1. The results show an improvement in V_{oc} as the CdCl_2 deposition time was increased, whereas little change in J_{sc} was observed to occur. Comparison to the reference ultra-thin device and a baseline device (CdTe = 2.25 μm) has also been made. It is clear that the V_{oc} drops significantly as the absorber thickness is reduced from the baseline to the ultra-thin CdTe. The large degree to which V_{oc} falls may suggest additional mechanisms to the effects of CdCl_2 treatment, such as back surface recombination [14], which is not addressed in this paper. Table 2 shows mean J – V parameters for the devices with best cells represented in Fig. 1.

Ultra-thin solar cells can suffer from a large variation in shunt resistance (R_{sh}) due to the presence of pin-holes from incomplete CdTe coverage. However, Table 2 shows similar FF values between the CdCl_2 treated ultra-thin cells suggesting little variation in R_{sh} between the ultra-thin PV cells. The reference ultra-thin cell has a more significant reduction in FF , which is attributed to the absence of CdCl_2 activation treatment. This showed some effect on series resistance (R_s), which increased, but may also be due to an increase in reverse saturation current density.

EQE of a cell from each sample is shown below in Fig. 2. In general, as previously reported [15], the window layer absorption edge shifts further into the blue region of the solar spectrum as the CdCl_2 deposition was reduced. This has a direct correlation to the level of Zn in the $\text{Cd}_{1-x}\text{Zn}_x\text{S}$ alloy detected by XPS. There is a discrepancy between samples T080A10 and T080A02, which had the same levels of CdCl_2 , but different anneal times. Sample T080A10, which was annealed for

Table 2
 J – V parameters for the ultra-thin CdTe PV cells represented by the J – V curves shown in Fig. 1.

Device	η (%)	J_{sc} (mA/cm^2)	V_{oc} (mV)	Anneal (s)
Baseline	13.5	23.8	808	70.1
Reference	2.7	11.8	485	48.0
T179A10	7.0	18.9	586	63.5
T120A10	6.3	17.6	566	63.1
T080A10	6.2	18.9	566	62.3
T080A02	6.4	18.9	525	64.7

Download English Version:

<https://daneshyari.com/en/article/8033992>

Download Persian Version:

<https://daneshyari.com/article/8033992>

[Daneshyari.com](https://daneshyari.com)